

# DNA-Binding Protein Nanotubes: Learning from Nature's Nanotech Examples

Gerald F. Audette, Erin J. van Schaik, Bart Hazes, and Randall T. Irvin\*

Department of Medical Microbiology & Immunology, University of Alberta,  
Edmonton, AB, Canada, T6G 2H7

Received July 6, 2004; Revised Manuscript Received August 18, 2004

## ABSTRACT

Bacterial pili are nanofibers made of protein subunits. Here we report the controlled assembly of protein nanotubes from an engineered *Pseudomonas aeruginosa* type IV pilin monomer. The nanotubes are up to 100  $\mu\text{m}$  long with an outer diameter of  $\sim 6$  nm and a predicted inner diameter of  $\sim 2$  nm. Protein nanotube formation appears to proceed through a hydrophobe-initiated conformational shift in the pilin monomer, which then self-associates to form thin linear filaments that coalesce to form long protein nanotubes. Protein nanotubes are highly attractive for nanotechnology, as protein engineering confers unprecedented control over mechanical and chemical properties. Moreover, like type IV pili, our nanotubes bind DNA, further broadening their appeal in nanotechnological applications.

Nanodevice fabrication requires the integration of both structure and function. Carbon nanotubes are useful in this respect as they have a regular linear structure and their surface chemistry can be modulated through chemical derivatization.<sup>1–5</sup> Indeed, the organized assembly and derivitization of carbon nanotubes has resulted in nanotechnology applications such as nanoelectronics<sup>6</sup> and biomolecular probes.<sup>7</sup> However, the extreme conditions needed to prepare carbon nanotubes<sup>4,8</sup> preclude the direct incorporation of many sensitive biological compounds, and control of the spatial distribution of functional groups through chemical derivitization is limited. Building nanotubes from proteins is attractive due to the rich structural and functional architectures that can be created. Indeed, cells routinely produce complex nanoscale functional structures such as flagella and pili (fiber-like protein polymers produced by a wide range of bacteria). Unfortunately, in vitro generation of such structures is not normally feasible as their synthesis requires complex multiprotein assembly machineries.<sup>9</sup> Here we report the first in vitro assembly of a protein nanotube from an engineered type IV pilin of *Pseudomonas aeruginosa*. The nanotubes resemble the type IV pilus of this organism in their structure as well as their ability to bind DNA.

Type IV pilins are  $\sim 15$  kDa proteins consisting of an antiparallel  $\beta$ -sheet, packed onto a long N-terminal  $\alpha$ -helix.<sup>10,11</sup> The N-terminal half of the  $\alpha$ -helix is highly hydrophobic, protrudes from the rest of the protein, and forms the core of the pilus fiber in all current assembly models,

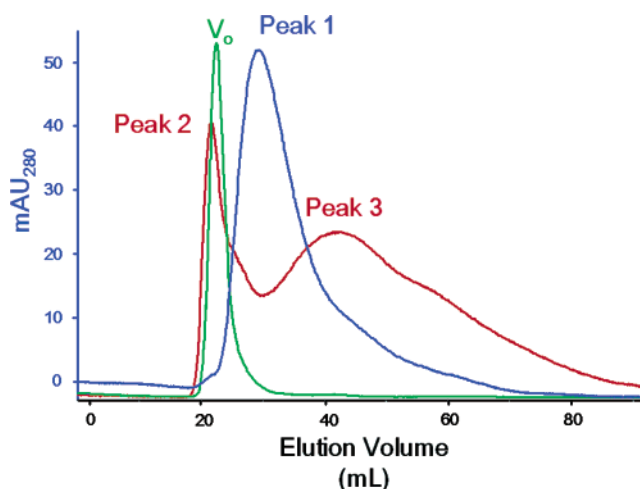


**Figure 1.** Chromatographic observation of monomeric and hydrophobe-triggered oligomerized  $\Delta\text{K122-4}$  pilin. Monomeric  $\Delta\text{K122-4}$  pilin unexposed to the  $\text{C}_{11}\text{-SH}$  hydrophobe (blue curve) eluted with a single peak (Peak 1). After exposure to the  $\text{C}_{11}\text{-SH}$  (red curve), a new  $\Delta\text{K122-4}$  peak (Peak 2) elutes in the void volume of the column as determined by the blue dextran high molecular weight marker (green curve). In addition to the high molecular weight peak, a second new peak at a longer retention volume (Peak 3) was observed in the  $\text{C}_{11}\text{-SH}$  exposed  $\Delta\text{K122-4}$  sample.

while the  $\beta$ -sheet forms the surface of the fiber.<sup>10–13</sup> Recently, we have engineered a truncated form of the pilin monomer from *P. aeruginosa* strain K122–4 where the first 28 exposed hydrophobic residues are deleted.<sup>13–15</sup> The resultant truncated pilin ( $\Delta\text{K122-4}$ ) is highly soluble, and NMR spectra and sedimentation equilibrium centrifugation analysis

\* Corresponding author. E-mail: randy.irvin@ualberta.ca.

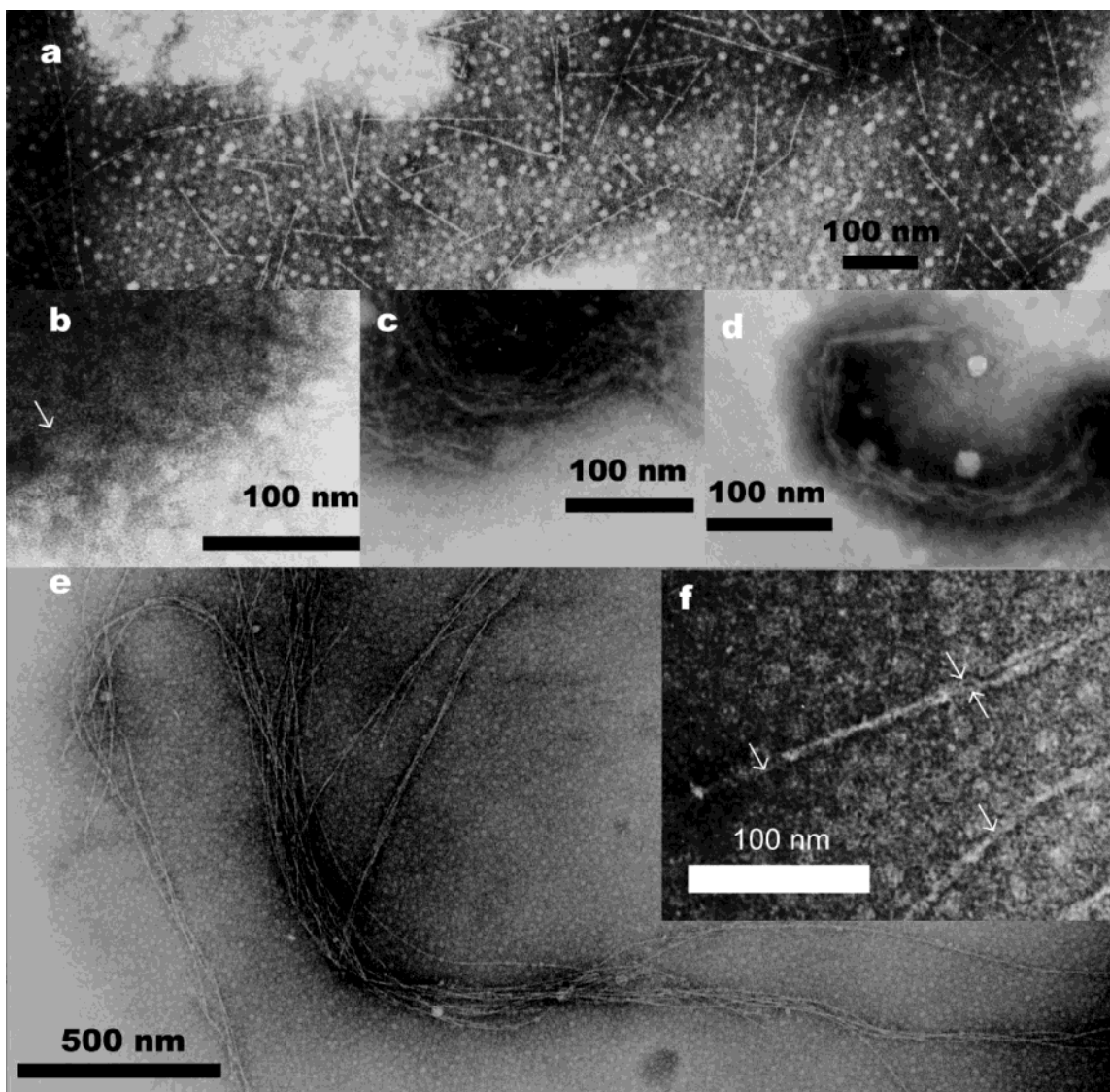


**Figure 2.** (a) Negatively stained purified *P. aeruginosa* pili. (b) Negatively stained hydrophobe treated monomeric pilin eluted from a Sephadex G50 SEC column (see Figure 1) as freshly eluted Peak 3. Note the material is largely unstructured monomeric protein with some very limited filament formation (arrow). (c) Peak 3 material that has been maintained at 4 °C for several hours is observed to contain significant quantities of thin linear filaments. (d) Peak 3 that has been maintained at 4 °C overnight now contains material that is aggregating into larger fibers. (e) Negatively stained nanotubes from Peak 2 (Figure 1); note the extreme length of the nanotubes. The diameter of the nanotubes in these micrographs is ~6 nm. (f) Higher magnification image of protein nanotubes indicating that the tubes occasionally “fray” into thin filaments (arrows), suggesting that the nanotubes consist of a multistart helical assembly of filaments. Samples were negatively stained with 1% aqueous ammonium molybdate (pH 7.0) and analyzed on an Hitachi H-7000 transmission electron microscope, operating at an accelerating voltage of 75 kV.

showed no evidence of aggregation, even at concentrations of 20 mg/mL or greater.<sup>13</sup> Despite its solubility, we observed that the protein sample aggregated on Superdex but not on Sephadex size exclusion chromatography (SEC) columns (Amersham Biosciences). Superdex resins contain dextran cross linked to agarose, making it more hydrophobic than Sephadex. To test for hydrophobe-triggered aggregation, we preincubated 15  $\mu$ L of 1.1 M 1-undecanethiol ( $C_{11}$ -SH, Aldrich) in methanol containing 1  $\mu$ M DTT and 1 mM EDTA at pH 6.4 with a 100  $\mu$ L aliquot of 10 mg/mL  $\Delta$ K122-4, followed by SEC analysis on a Sephadex G50 column. Figure 1 shows that untreated monomeric  $\Delta$ K122-4 elutes as expected for a protein of this size on the Sephadex column (Peak 1), while  $\Delta$ K122-4 exposed to  $C_{11}$ -SH elutes

within the void volume of the column (Peak 2; the void volume of the column was determined using Blue Dextran 2000). In addition, a new peak with a longer retention time than that of the untreated sample appeared in the  $C_{11}$ -SH treated pilin sample (Peak 3). MALDI-ToF MS of both Peaks 1 and 3 yielded a mass of 12837.57 Da, close to the predicted value of 12833.37 Da for the  $\Delta$ K122-4 monomer. In contrast, Peak 2 did not show any clear MS peaks within the 2–100 kDa detection limits of the instrument (data not shown). Therefore, the Peak 2 fraction appears to contain a MS-stable complex of more than 8 pilin monomers. Peak 3’s increased retention time without a change in molecular mass indicates a noncovalent alteration of the pilin monomer. Most likely this altered pilin monomer elutes more slowly

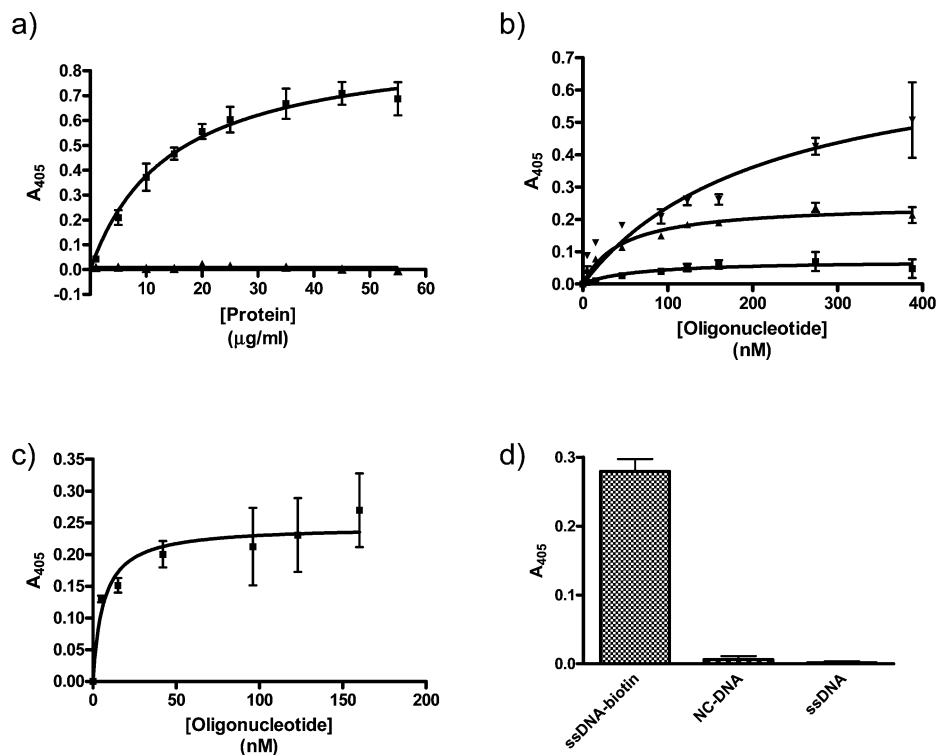


**Figure 3.** (a) Concentration-dependent binding of  $\Delta\text{K122-4}$  pilin to the  $\text{C}_{11}\text{-SH}$  hydrophobe. The interaction of  $\Delta\text{K122-4}$  pilin (squares) versus ovalbumin (triangles) with the hydrophobe was monitored using a cross-reactive polyclonal anti-pilin antibody.<sup>19,20</sup> Data shown are the mean of 4 trials  $\pm$  SD. (b) Binding of biotinylated DNA by immobilized K122-4 pili (inverted triangles),  $\Delta\text{K122-4}$  nanotubes (triangles), and  $\Delta\text{K122-4}$  monomer (squares). Data shown are the mean of 3 trials  $\pm$  SD and for the  $\Delta\text{K122-4}$  nanotubes; 123 nM of oligonucleotide was found to be saturating. (c) Immobilized  $\Delta\text{K122-4}$  nanotubes incubated with unlabeled oligonucleotide (123 nM) are able to capture a biotinylated oligonucleotide of complimentary sequence. Data shown are the mean of 3 trials  $\pm$  SD. (d)  $A_{405}$  measurements of binding of biotinylated (ssDNA-biotin) and unlabeled (ssDNA) at saturating concentrations to immobilized nanotubes. Preincubation of nanotubes with DNA of a sequence noncomplimentary to that of the biotinylated probe (NC-DNA) at 123 nM prevents nanotube capture of the biotinylated probe.

due to interaction with the resin resulting from either a hydrophobe-induced conformational change or direct binding of the hydrophobe. It is possible that Peak 3 represents an intermediate form from which the high molecular weight Peak 2 material is formed as prolonged storage of this peak at ambient temperature or 4 °C results in the oligomerization of very large molecular aggregates.

Given that the oligomerized material in Peak 2 remained soluble, we hypothesized that it might form pilus-like fibers rather than random aggregates. To test this, samples from Peaks 2 and 3 as well as untreated monomeric  $\Delta\text{K122-4}$  were negatively stained with 1% aqueous ammonium molybdate (pH 7.0) and analyzed by electron microscopy (EM; Hitachi H-7000 instrument; operating at an accelerating voltage of 75 kV). The protein in Peak 2 clearly forms pilus-like fibers (Figure 2e) with lengths up to 100  $\mu\text{m}$  and a diameter of 5–6 nm (these fibers are much longer than classically purified *P. aeruginosa* pili, cf. Figures 2a and 2e), whereas EM analysis of either freshly eluted Peak 3 (Figure 2b) or untreated monomeric pilin (not shown) showed no evidence of pilus-like structures. Interestingly, our nanotube EM images closely resemble those of natural type IV pili (Figure 2a,e,f),<sup>16</sup> but differ from  $\beta$ -amyloid fibers.<sup>17</sup>  $\beta$ -amyloid fibers can be stained with the dye Congo Red;<sup>18</sup> however, our protein nanotubes did not bind Congo Red (not shown), supporting the hypothesis that the  $\Delta\text{K122-4}$

monomers maintain a native-like conformation. While Peak 3 initially elutes as unstructured monomeric protein, over time the protein self-assembles into thin ( $\sim 2$  nm diameter) linear filaments of variable length (Figure 2c) that then coalesce into fibers (Figure 2d) and eventually long nanotubes (Figure 2e). Close examination of negatively stained nanotubes (Figure 2f) suggests that the nanotubes self-assemble from the thin linear filaments in a helical manner to generate hollow nanotubes. Nanotubes occasionally “fray” into thin filaments (Figure 2f, arrows), further supporting a multistart helical assemblage of filaments into nanotubes model.

As the oligomerization of  $\Delta\text{K122-4}$  pilin in solution was initiated by the addition of a hydrophobe, we wished to determine if the  $\Delta\text{K122-4}$  monomer could interact with a surface constrained hydrophobe. Increasing concentrations of  $\Delta\text{K122-4}$  (0–55  $\mu\text{g/ml}$ ) were added to  $\text{C}_{11}\text{-SH}$  (49 ng) covalently attached to maleimide-activated microtiter plates, and interaction of the pilin was monitored immunologically<sup>19</sup> using polyclonal sera generated against the *P. aeruginosa* strain K pili known to be cross reactive to pili from several *P. aeruginosa* strains.<sup>20</sup> When  $\Delta\text{K122-4}$  was incubated in the presence of surface constrained  $\text{C}_{11}\text{-SH}$ , a concentration dependent binding of the pilin to the hydrophobe was observed (Figure 3a). This observation, coupled with the aggregation and clogging of hydrophobic matrices and the

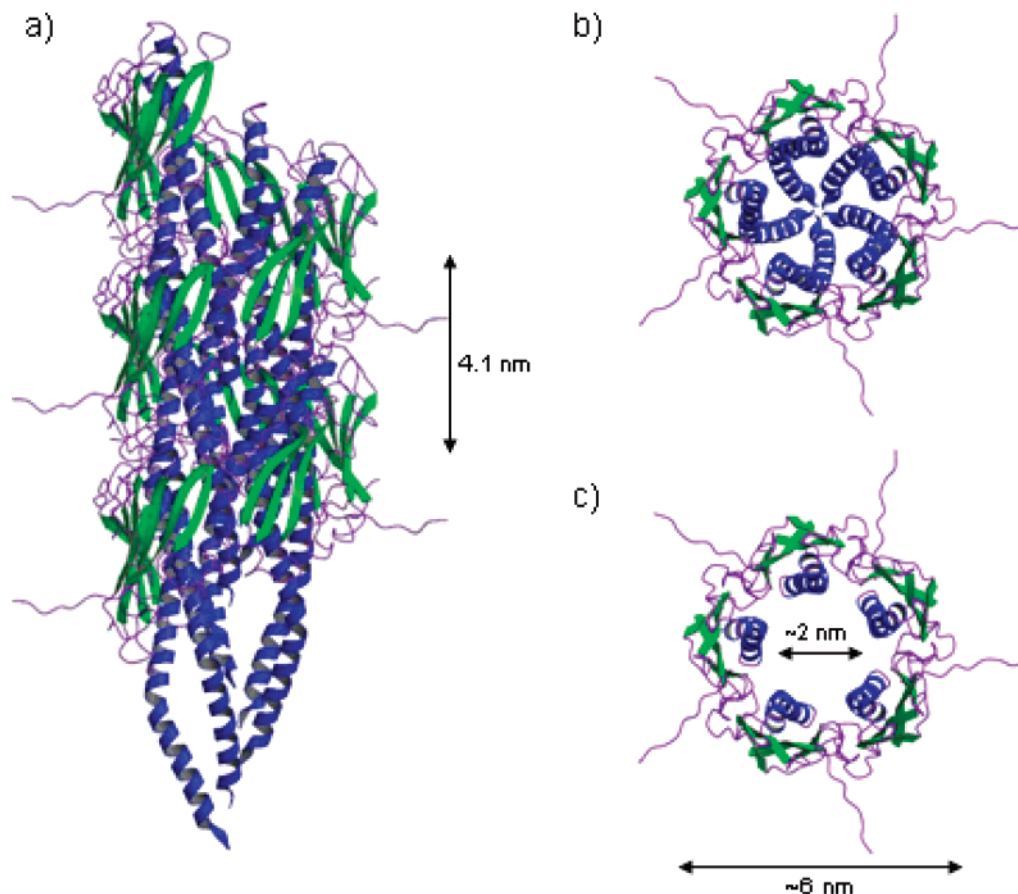


**Figure 4.** Type IV pili and protein nanotubes. (a) Two turns of a type IV pilus assembled from the  $\Delta$ K122–4 pilin with the addition of the 28 N-terminal residues of the *N. gonorrhoeae* MS11 pilin,<sup>10</sup> known to be the closest structural homologue to K122–4,<sup>15</sup> using the assembly parameters of Parge et al.<sup>10</sup> Models of type IV pili are based on fiber diffraction<sup>21</sup> and EM studies, which indicate that type IV pili contain a 4.1 nm helical pitch and outer diameter of  $\sim$ 6 nm. For each pilin monomer, the N-terminal  $\alpha$ -helix is blue, the 4-stranded antiparallel  $\beta$ -sheet is green, and loop regions are purple. (b) Axial view of a single turn of the type IV pilus from (a). Note that the central core of the pilus is occupied by the N-terminal hydrophobic helices of the pilin monomers. (c) Axial view of the protein nanotubes, constructed from  $\Delta$ K122–4 pilin monomers. The removal of the N-terminal  $\alpha$ -helix in the pilin monomer results in the generation of an  $\sim$ 2 nm hydrated central core. This figure was produced using Molscript and Raster3D.<sup>27</sup>

change in relative mobility of  $\Delta$ K122–4 monomer on Sephadex G50 following exposure to hydrophobe (Figure 1), suggests that the C<sub>11</sub>–SH hydrophobe is only needed to trigger  $\Delta$ K122–4 oligomerization.

Type IV pili are multifunctional structures that are able to bind to diverse surfaces and substrates. We have recently observed that the type IV pili from several strains of *P. aeruginosa* bind directly to both double-stranded DNA and single-stranded DNA (van Schaik et al., submitted). We therefore examined the possibility that the protein nanotubes could also bind DNA. Ten micrograms of  $\Delta$ K122–4 monomer or nanotubes were coated on 96-well microtiter plates and increasing concentrations of the oligonucleotide Biotin-ACTCGCCGTCTGAACCTA (0–388 nM) was added. The  $\Delta$ K122–4 nanotubes bind single-stranded DNA with moderate affinity and an apparent  $K_d$  of  $\sim$ 46 nM; 123 nM of oligonucleotide was found to be saturating (Figure 3b). Monomeric protein only marginally bound the ssDNA oligonucleotide (Figure 3b). Furthermore, a nonbiotinylated nanotube-bound oligonucleotide (123 nM) was able to specifically capture a biotinylated anti-sense DNA probe (Figure 3c).

The similarity in structure, DNA-binding properties, and antibody recognition suggests that our truncated  $\Delta$ K122–4 pilin assembles into a protein nanotube that closely resembles the natural type IV pilus fiber. This is surprising since the hydrophobic N-terminal half of the  $\alpha$ -helix, the part that we deleted, has generally been believed to play an important role in pilus assembly and structural stability. Several models of type IV pili have been created by combining results from fiber diffraction,<sup>21</sup> biochemical data, and the three-dimensional structures of *Neisseria gonorrhoeae* MS11 pilin,<sup>10</sup> the toxin-coregulated pilin from *Vibrio cholerae*,<sup>11</sup> and pilins from *P. aeruginosa* strains K (PAK)<sup>12</sup> and K122–4<sup>13</sup> (Figure 4). The models differ considerably in their assembly arrangement (1-, 3-, and 5-start helix models have been proposed); however, in all models the hydrophobic N-terminal half of the  $\alpha$ -helix forms the core of the fiber (Figure 4a,b). The measured diameter of the protein nanotubes is the same as that observed for PAK pili, and when pilus models of the same filament diameter are constructed from our truncated pilin monomer, each nanotube model (1-, 3-, or 5-start helix) would contain a hydrated inner cavity of  $\sim$ 2 nm in diameter (Figure 4c). The somewhat lower contrast

of the nanotubes with respect to the native pili supports this hypothesis (compare Figures 2a and 2f). Also, the mechanical strength of the natural MS11 pili exceeds 100 pN.<sup>22</sup> While the tensile strength of our nanotubes remains unknown, their long length (Figure 2e) indicates that they are relatively robust and can resist hydrodynamic shear forces, possibly by localized unwinding of the intertwined pilin filaments.

The assembly of type IV pili requires a complex protein apparatus that is related to the type II protein secretion pathway.<sup>9</sup> Interestingly, type IV pilus assembly machinery of one bacterial strain can produce functional pili from highly divergent pilin subunits having very different amino acid sequences.<sup>23</sup> This suggests that the assembly involves a common mechanism that tolerates significant sequence variation. The conservation of the *in vivo* assembly process is believed to be due to the hydrophobic N-terminal half of the  $\alpha$ -helix, as it is the most conserved feature shared by all type IV pilins.<sup>12</sup> It is possible that *in vitro* nanotube assembly is initiated by interaction with a hydrophobic compound that acts as a surrogate for the hydrophobic  $\alpha$ -helix, which we have deleted from the monomeric protein. The nature of the hydrophobe does not, however, appear to be important as Superdex resin, C<sub>11</sub>-SH, as well as other hydrophobes (not shown) can trigger nanotube formation. Also, our observation that  $\Delta$ K122-4 can interact with a surface constrained hydrophobe (Figure 3a) suggests that the hydrophobe does not need to be incorporated into the nanotube, but merely serves as a nucleation point for self-assembly. Interaction between  $\Delta$ K122-4 and hydrophobe could induce a conformational change in the protein that allows for the monomers to self-associate to form thin filaments. These thin filaments then spontaneously interact in a helical fashion (a multistart helix) to generate the long protein nanotubes. Future research into pilin nanotube formation should clarify the mechanism of nanotube assembly and help to understand the assembly of type IV pili *in vivo*.

The self-assembly of nanostructures from biological systems is of great interest. It has been reported recently that nanotubes and nanofibers have been generated from cyclic peptides<sup>24</sup> and amphiphilic synthetic peptides.<sup>25</sup> Amyloid fibers have also been reported to form water-filled nanotubes.<sup>17</sup> To our knowledge, we present here the first evidence of a self-assembling nanotube from a soluble globular protein subunit. Our protein nanotubes have several properties that make them well suited for developments in nanotechnology. Functional pili are formed from a wide diversity of pilin monomers with high sequence variation.<sup>12,23</sup> Accordingly, the system should allow us to use protein engineering to add desirable functionalities and modify strength, rigidity, or other physical properties. The DNA binding activity can be used as an adaptor technology to coat the nanotubes with various (bio)chemical moieties. For example, nanotube-bound biotinylated-DNA (either single or double stranded) may be employed to capture target molecules that are coupled to streptavidin. If the nanotubes were to bind M-DNA, a novel current-conducting form of DNA with bound divalent metal ions,<sup>26</sup> then it may be possible to create a mixed protein/DNA-based nanowire. Finally, if nanotube formation

can be nucleated on a hydrophobic surface, as suggested by the aggregation of pilin monomers on hydrophobic matrices and surface constrained C<sub>11</sub>-SH (Figure 3a), it should be possible to restrict nanotube assembly to certain locations by presenting hydrophobes at these locations only. Research is underway to study the application of this potential and provide insight into the structure and assembly mechanism of both the nanotube and the natural type IV pilus.

**Acknowledgment.** Technical assistance by A. M. Brigley, M. Kaplan, and L. M. Price is gratefully acknowledged. This work was supported by operating grants from the Canadian Institutes for Health Research operating grants to B.H. (MOP-42448) and R.T.I. (MOP-38004).

**Supporting Information Available:** Details concerning protein nanotube assembly and analysis. Experimental procedures for protein nanotube assembly in solution, size exclusion chromatography, concentration dependent binding of  $\Delta$ K122-4 pilin to C<sub>11</sub>-SH, DNA binding and DNA capture assays. This material is available free of charge via the Internet at <http://pubs.acs.org>.

## References

- (1) Ajayan, P. M.; Charlier, J.-C.; Rinzler, A. G. *Proc. Natl. Acad. Sci. U.S.A.* **1999**, *96*, 14199–14200.
- (2) Dwyer, C.; Guthold, M.; Falvo, M.; Washburn, S.; Superfine, R.; Erie, D. *Nanotechnology* **2002**, *13*, 601–604.
- (3) Georgakilas, V.; Kordatos, K.; Prato, M.; Guldi, D. M.; Holzinger, M.; Hirsch, A. *J. Am. Chem. Soc.* **2002**, *124*, 760–761.
- (4) Ajayan, P. M. *Chem. Rev.* **1999**, *99*, 1787.
- (5) Wei, B. Q.; Vajtai, R.; Jung, Y.; Ward, J.; Zhang, R.; Ramanath, G.; Ajayan, P. M. *Nature* **2002**, *416*, 495.
- (6) Tans, S. J.; Veshueren, A. R. M.; Dekker, C. *Nature* **1998**, *393*, 49–52.
- (7) Wong, S. S.; Joselevich, E.; Woolley, A. T.; Cheung, C. L.; Lieber, C. M. *Nature* **1998**, *394*, 52–55.
- (8) Zhu, H. W.; Xu, C. L.; Wu, D. H.; Wei, B. Q.; Vajtai, R.; Ajayan, P. M. *Science* **2002**, *296*, 884–886.
- (9) Mattick, J. S. *Annu. Rev. Microbiol.* **2002**, *56*, 289–314. Remaut, H.; Waksman, G. *Curr. Opin. Struct. Biol.* **2004**, *14*, 161–170.
- (10) Parge, H. E.; Forest, K. T.; Hickey, M. J.; Christensen, D. A.; Getzoff, E. D.; Tainer, J. A. *Nature* **1995**, *378*, 32–38.
- (11) Craig L.; Taylor, R. K.; Pique, M. E.; Adair, B. D.; Arvai, A. S.; Singh, M.; Lloyd, S. J.; Shin, D. S.; Getzoff, E. D.; Yeager, M.; Forest, K. T.; Tainer, J. A. *Mol. Cell* **2003**, *11*, 1139–1150.
- (12) Hazes, B.; Sastry, P. A.; Hayakawa, K.; Read, R. J.; Irvin, R. T. *J. Mol. Biol.* **2000**, *299*, 1005–1017.
- (13) Keizer, D. W.; Slupsky, C. M.; Kalisiak, M.; Campbell, A. P.; Crump, M. P.; Sastry, P. A.; Hazes, B.; Irvin, R. T.; Sykes, B. D. *J. Biol. Chem.* **2001**, *276*, 24186–24193.
- (14) Audette, G. F.; Irvin, R. T.; Hazes, B. *Acta Crystallogr.* **2003**, *D59*, 1665.
- (15) Audette, G. F.; Irvin, R. T.; Hazes, B. *Biochemistry* **2004**, *43*, 11427–11435.
- (16) Lee, K. K.; Sheth, H. B.; Wong, W. Y.; Sherbourne, R.; Paranchych, W.; Hodges, R. S.; Lingwood, C. A.; Krivan, H.; Irvin, R. T. *Mol. Microbiol.* **1994**, *11*, 705–713.
- (17) Perutz, M. F.; Finch, J. T.; Berriman, J.; Lesk, A. *Proc. Natl. Acad. Sci. U.S.A.* **2002**, *99*, 5591–5595.
- (18) Klunk, W. E.; Jacob, R. F.; Mason, R. P. *Methods Enzymol.* **1999**, *309*, 285–305.
- (19) Doig, P.; Todd, T.; Sastry, P. A.; Lee, K. K.; Hodges, R. S.; Paranchych, W.; Irvin, R. T. *Infect. Immun.* **1998**, *56*, 1641–1646. Schweizer, F.; Jiao, H.; Hindsgaul, O.; Wong, W. Y.; Irvin, R. T. *Can. J. Microbiol.* **1998**, *44*, 307–311.
- (20) Sheth, H. B.; Glasier, L. M.; Ellert, N. W.; Cachia, P.; Kohn, W.; Lee, K. K.; Paranchych, W.; Hodges, R. S.; Irvin, R. T. *Biomed. Pept. Proteins Nucleic Acids* **1995**, *1*, 141–148.
- (21) Folkhard, W.; Marvin, D. A.; Watts, T. H.; Paranchych, W. *J. Mol. Biol.* **1981**, *149*, 79–93. Marvin, D. A.; Nadassy, K.; Welsh, L. C.; Forest, K. T. *Fibre Diffraction Rev.* **2003**, *11*, 87–94.

- (22) Merz, A. J.; So, M.; Sheetz, M. P. *Nature* **2000**, *407*, 98–102. Maier, B.; Potter, L.; So, M.; Seifert, H. S.; Sheetz, M. P. *Proc. Natl. Acad. Sci. U.S.A.* **2002**, *99*, 16012–16017.
- (23) Watson, A. A.; Mattick, J. S.; Alm, R. A. *Gene* **1996**, *175*, 143–150.
- (24) Hartgerink, J. D.; Granja, J. R.; Milligan, R. A.; Ghadiri, M. R. *J. Am. Chem. Soc.* **1996**, *118*, 43–50. Kim, H. S.; Hartgerink, J. D.; Ghadiri, M. R. *J. Am. Chem. Soc.* **1998**, *120*, 4417–4424.
- (25) Hartgerink, J. D.; Clark, T. D.; Ghadiri, M. R. *Chem. Eur. J.* **1998**, *4*, 1367–1372. Hartgerink, J. D.; Beniash, E.; Stupp, S. I. *Science* **2001**, *294*, 1684–1688. Hartgerink, J. D.; Beniash, E.; Stupp, S. I. *Proc. Natl. Acad. Sci. U.S.A.* **2002**, *99*, 5133–5138.
- (26) Aich, P.; Labiuk, S. L.; Tari, L. W.; Delbaere, L. T. J.; Roesler, W. J.; Falk, K. J.; Steer, R. P.; Lee, J. S. *J. Mol. Biol.* **1999**, *294*, 477–485. Rakitin, A.; Aich, P.; Papadopoulos, C.; Kobzar, Y.; Vedeneev, A. S.; Lee, J. S.; Xu, J. M. *Phys. Rev. Lett.* **2001**, *86*, 3670–3673. Aich, P.; Skinner, R. J.; Wettig, S. D.; Steer, R. P.; Lee, J. S. *J. Biomol. Struct. Dyn.* **2002**, *20*, 93–98. Wettig, S. D.; Li, C.-Z.; Long, Y.-T.; Kraatz, H.-B.; Lee, J. S. *Anal. Sci.* **2003**, *19*, 23–26.
- (27) Kraulis, J. J. *Appl. Cryst.* **1991**, *24*, 946–950. Merritt, E. A.; Bacon, D. J. *Methods Enzymol.* **1997**, *277*, 505–524.

NL048942F